

# The Compensation of Coarseness Error in 2D TLM Modeling of Microwave Structures

U. Mueller, P. P. M. So and W. J. R. Hoefer

University of Ottawa, Dept. of Electrical Eng., 161 Louis Pasteur, Ottawa, Ontario K1N 6N5, Canada

## Abstract

In this paper the origin of the coarseness error in two-dimensional TLM meshes is investigated, and a method for compensating the coarseness effect without increasing the computational expenditure is presented. The efficiency and accuracy of this method is demonstrated by comparison with analytically exact solutions.

## Introduction

It can be observed in all TLM computations that results are invariably shifted towards lower frequencies, particularly when the structure under study has sharp edges or corners. This phenomenon has already been described by Shih and Hoefer in the analysis of Fin-lines with the 2D-TLM method [1]. The effect was called the coarseness error and attributed to the lack of resolution of highly nonuniform electromagnetic fields by the discretization [1, 2, 3]. In this paper the nature of this coarseness error will be investigated in more detail, and methods for compensating the coarseness error without increasing the computational expenditure will be presented.

## Theoretical Background

TLM analysis of structures containing sharp corners is always affected by considerable coarseness error. For example, when the effective dielectric constant in transmission lines or waveguides with  $360^\circ$  or  $270^\circ$  edges is computed, TLM results are always lower than predicted by theory.

This error is mainly due to the fact that at sharp corners there are nodes which are closer than  $\Delta l$  to the boundaries, but have no branch connected directly to

them, as shown in Fig. 1. While nodes *C* and *D* are directly connected to the conducting boundary, nodes *A* and *B* are not, even though they are in "territorial waters". The "information distance" between nodes *A*, *B* and the conductor is  $3\Delta l/2$  along the paths *ACE*, *BDE* and *ADF* rather than  $\Delta l/(2\sqrt{2})$ , the shortest distance *AG* and *BG*.

The interaction with the boundary of nodes *A* and *B* is thus delayed by two time steps, which leads to nonphysical field behaviour around the edge, resulting in reactive energy storage and, hence, an increase in the effective dielectric constant of a structure. This is the reason why the discrete system cannot represent the highly nonuniform field in the vicinity of such edges with appropriate accuracy, and it is the principal source of the so-called coarseness error. This effect disappears when the mesh parameter  $\Delta l$  becomes infinitesimal. In the following, a method for improving the edge behaviour of TLM will be proposed.

## Directional Compensation

In order to establish a direct link between a corner node and the boundary it is proposed to add a fifth branch as shown in Fig. 2. The corner node itself is shown enlarged in Fig. 3. The fifth arm is  $l'$  long, runs at  $45^\circ$  with respect to the regular arms 1 and 4, and is terminated at its extremity by the boundary condition imposed by the corner.

We can now apply various considerations to determine the characteristic admittance of the branches and hence, the impulse scattering matrix of this special node.

For reasons of symmetry we must have

$$Y_1 = Y_4 \quad , \quad (1)$$

and furthermore

$$Y_3 = Y_2 \quad . \quad (2)$$

The node itself should exhibit an admittance continuity in diagonal direction (direction of branch 5) for the reason that energy must be partitioned between the branches in such a way that it is scattered equally in all directions, as postulated in Huygens's original model. Hence

$$Y_2 + Y_3 = Y_1 + Y_4 + Y_5 . \quad (3)$$

However, nothing is known yet about the distribution of the energy among the branches 1, 4 and 5. One can only say that for reasons of symmetry the energy carried by branches 1 and 4 should be the same. Let us assume for the moment that branch 5 carries a fraction  $p$  of the total energy scattered into the branches 1, 4 and 5.

Finally we must consider that for reasons of synchronism, impulses on branch 5 must travel  $\psi$ -times faster than those on the other branches, with  $\psi = \frac{l'}{\Delta l/2} = \sqrt{2}$  for an ideal corner, while the velocity in the branches 1 to 4 should be the same as in the regular node branches.

Under these assumptions we can find the normalized admittances of the corner node branches to be

$$\begin{aligned} y_1 = y_4 &= 1 - p & ; \quad y_2 = y_3 = 1 \\ y_5 &= 2p \end{aligned}$$

where the exact value of  $p$  remains to be determined.

Since branches 1, 4 and 5 have characteristic admittances different from those of the remaining mesh lines, ideal transformers must be inserted between them (Fig. 3(b)) and the TLM mesh to avoid scattering at the connection points.

Once these impedance transformers have been introduced into the impulse scattering equation, the scattering matrix  $[S]$  for the vectors of incident and reflected voltages  $[V]^i$  and  $[V]^r$  at the outer terminals of the ideal transformers can be written in the following form:

$$[S] = \begin{bmatrix} a & \frac{1}{2n_b} & \frac{1}{2n_b} & b & \frac{n_c d}{n_b} \\ n_b b & -\frac{1}{2} & \frac{1}{2} & n_b b & n_c d \\ n_b b & \frac{1}{2} & -\frac{1}{2} & n_b b & n_c d \\ b & \frac{1}{2n_b} & \frac{1}{2n_b} & a & \frac{n_c d}{n_b} \\ \frac{n_c b}{n_b} & \frac{1}{2n_c} & \frac{1}{2n_c} & \frac{n_b b}{n_c} & c \end{bmatrix} \quad (4)$$

with the abbreviations

$$\begin{aligned} a &= -\frac{1+p}{2} & ; \quad b = 1 + a = \frac{1-p}{2} \\ c &= p-1 & ; \quad d = 1 + c = p \\ n_b &= \sqrt{\frac{1}{y_b}} & ; \quad n_c = \sqrt{\frac{1}{y_c}} \end{aligned} .$$

## Nondirectional Compensation

In the above procedure the admittances of the branches extending towards the corner or edge are modified. This means that not only the coordinates but also the relative position of a node with respect to the corner must be specified.

We have therefore studied the possibility to simply add a short-circuited  $\frac{\Delta l}{2}$  stub of normalized admittance  $y_5$  to the corner node without modifying the admittances of branches 1 to 4. This leads to a simpler scattering matrix  $[S]$ , which can be written as

$$[S] = \begin{bmatrix} e & f & f & f & g \\ f & e & f & f & g \\ f & f & e & f & g \\ f & f & f & e & g \\ f & f & f & f & h \end{bmatrix} \quad (5)$$

with the abbreviations

$$\begin{aligned} e &= \frac{-(2+y_5)}{4+y_5} & ; \quad f = \frac{2}{4+y_5} \\ g &= \frac{2y_5}{4+y_5} & ; \quad h = \frac{y_5-4}{4+y_5} \end{aligned}$$

This method requires only that the coordinates of the corner nodes be specified. Obviously the stub admittance  $y_5$  will be different from its value in the directional compensation case and remains to be determined.

## Determination of Corner Node Parameters

We have determined the corner node parameters by optimizing them for best compensation of the coarseness error in the resonant frequencies of the dominant and the first higher order mode of quarter-wave resonators containing  $270^\circ$  and  $360^\circ$  field singularities. Accurate resonant frequencies were obtained by a series of TLM computations using increasingly fine meshes and extrapolating these results for  $\Delta l \rightarrow 0$ , as described in [1]. Then, the same structures were computed with coarse meshes comprising corner nodes, and their parameters were optimized such that they yielded the accurate reference values.

The following values were obtained:

Corner Type	Directional Compensation ( $p_{opt}$ )	Nondirectional Compensation ( $y_{5,opt}$ )
$270^\circ$	0.115	0.181
$360^\circ$	0.105	0.167

It was found that these parameters were insensitive to meshsize, frequency and direction of propagation in the mesh within the usual limits for acceptable velocity error.

Fig. 4 to 6 demonstrate the effect of optimized coarseness error compensation for different corner node and edge types. It can be seen that the proposed techniques yield in all cases excellent results with considerably less computational effort than uncompensated TLM schemes having the same accuracy.

## Residual Errors

While the proposed method practically eliminates the major source of error (coarseness error), some lesser errors remain. These are the dispersion of the network [4] (which can be corrected as shown in [3]) and the truncation error [5] due to the restriction to a finite time domain response.

## Conclusions

We have demonstrated how the coarseness error in 2D-TLM simulations can be eliminated by modifying the properties of the nodes situated at sharp corners or edges. The compensation is achieved by adding reactive stubs to the corner nodes. As a result, relatively coarse TLM meshes may be used to obtain highly accurate results. The savings in computational expenditure are typically three orders of magnitude in 2D-TLM simulations.

## Acknowledgement

The Authors want to thank Professor P. Saguet of the Institut National Polytechnique de Grenoble, France, for numerous discussions on this subject.

## References

- [1] Y.-C. Shih and Hoefer, "Dominant and second-order mode cutoff frequencies with a two-dimensional TLM-program", *IEEE Trans. Microwave Theory Tech.*, vol. MTT-28, pp. 1443-1448, Dec. 1980.
- [2] Y.-C. Shih, "The analysis of fin lines using transmission line matrix and transverse resonance method", M. A. SC. Thesis, University of Ottawa, Canada, 1980.
- [3] W. J. R. Hoefer, "The transmission line matrix (TLM) method", in T. Itoh, "Numerical techniques for microwave and millimeter-wave passive structures", pp. 496-591, J. Wiley & Sons, New York 1989.
- [4] S. Akhtarzad, "Analysis of lossy microwave structures and microstrip resonators by the TLM method", Ph.D. Dissertation, University of Nottingham, England, July 1975.
- [5] P. B. Johns, "Application of the transmission line matrix method to homogeneous waveguides of arbitrary cross-section", *Proc. Inst. Electr. Eng.*, vol. 119, pp. 1086-1091, August 1972.

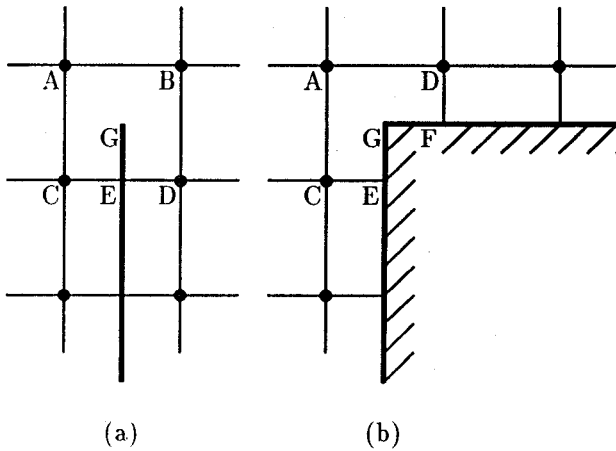


Figure 1: 2D-TLM network containing a  $360^\circ$  (a) and a  $270^\circ$  (b) edge.

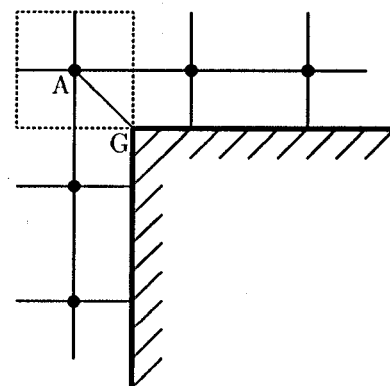


Figure 2: Corner node A with an additional corner arm

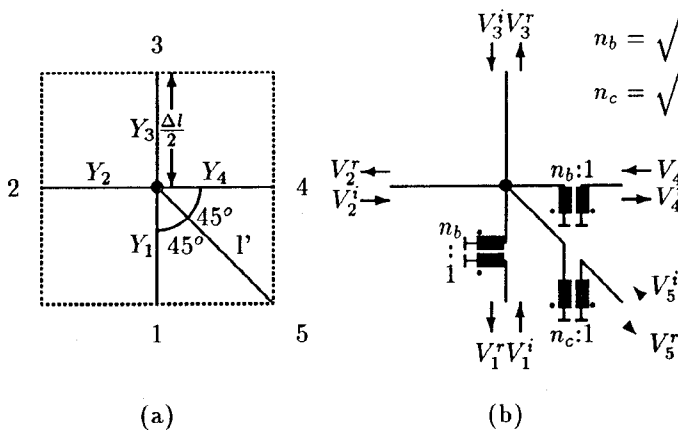


Figure 3: Corner node with a fifth arm at  $45^\circ$  having a length  $l'$ . (a) is an enlargement of the dotted box in Fig. 2 above, (b) shows the connection of the corner node to the TLM mesh via ideal impedance transformers (directional compensation).

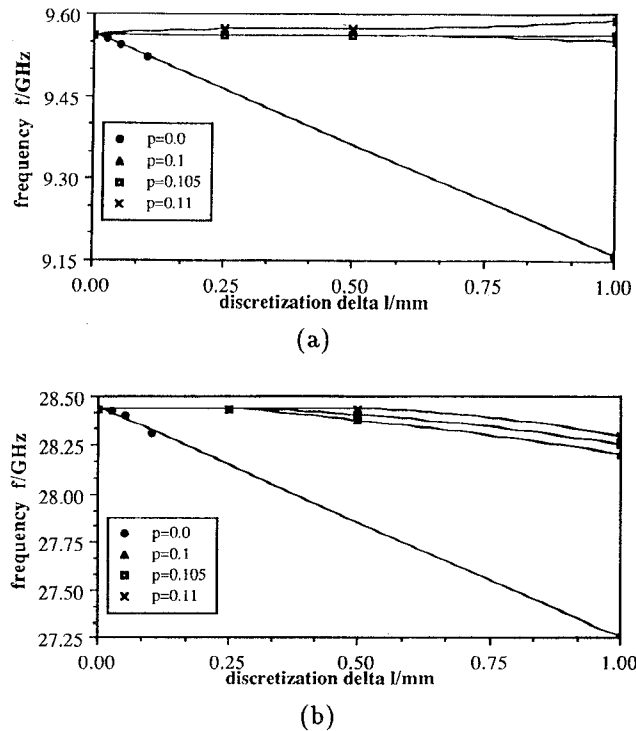


Figure 4: Effect of the directional compensation mechanism on the resonant frequencies of a structure with a  $360^\circ$  field singularity. (a) dominant mode resonance and (b) first higher order mode resonance versus discretization  $\Delta l$ . The parameter is  $p$ .

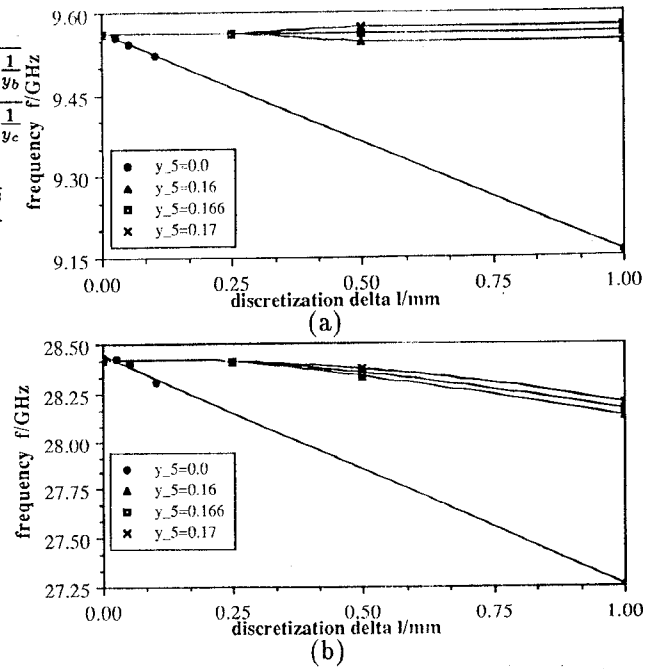


Figure 5: Effect of the nondirectional compensation mechanism on the resonant frequencies of a structure with a  $360^\circ$  field singularity. (a) dominant mode resonance and (b) first higher order mode resonance versus discretization  $\Delta l$ . The parameter is  $y_5$ .

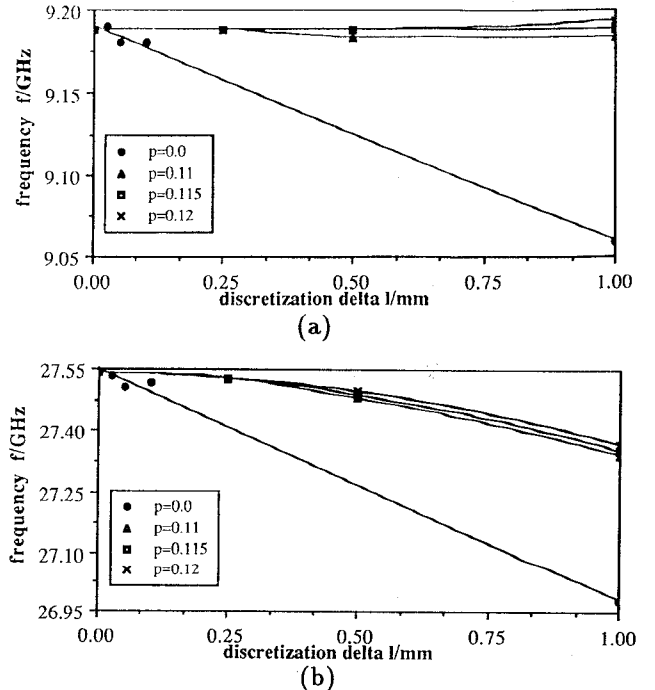


Figure 6: Effect of the directional compensation mechanism on the resonant frequencies of a structure with a  $270^\circ$  field singularity. (a) dominant mode resonance and (b) first higher order mode resonance versus discretization  $\Delta l$ . The parameter is  $p$ .